MODELING OF NS-LASER ABLATION: CALCULATIONS BASED ON A NON-STATIONARY AVERAGING TECHNIQUE (SPATIAL MOMENTS)

N. Arnold [a], B. Luk'yanchuk [b], N. Bityurin [c], and D. Bäuerle [a]

[a] Angewandte Physik, Johannes-Kepler-University, A-4040 Linz, Austria
[b] General Physics Institute, Russian Academy of Sciences, 117942 Moscow, Russia
[c] Institute of Applied Physics, Russian Academy of Sciences, 603600 Nizhnii Novgorod, Russia

ABSTRACT

Semi-analytical approach to a quantitative analysis of thermal ns laser ablation is presented. It permits one to take into account:
- arbitrary temperature dependences of material parameters, such as the specific heat, thermal conductivity, absorptivity, absorption coefficient, etc.
- arbitrary temporal profiles of the laser pulse.
- strong (Arrhenius-type) dependence of the ablation velocity on the temperature of the ablation front, which leads to a non-steady movement of the ablation boundary during the (single) pulse.
- screening of the incoming radiation by the ablated products.
- influence of the ablation (vaporization) enthalpy on the heating process.
- influence of melting and/or other phase transformations.

The nonlinear heat conduction equation is reduced to three ordinary differential equations which describe the evolution of the surface temperature, spatial width of the enthalpy distribution, and the ablated depth. Due to its speed and flexibility, the method provides powerful tool for the fast analysis of the experimental data.

The influence of different factors onto ablation curves (ablated depth h vs. fluence ϕ) is studied. Analytical formulas for ϕ_{th} and $h(\phi)$ dependences are derived and discussed. The ablation curves reveal three regions of fluence: Arrhenius region, linear region, and screening region. Threshold fluence ϕ_{th} and Arrhenius tails at $\phi < \phi_{th}$, are affected heavily by the temperature dependences in material parameters, surface evaporation rate, and pulse duration and shape. In contrast, the *slope* of the ablation curves at $\phi > \phi_{th}$, is determined almost exclusively by the latent heat of vaporization, high temperature dependence of absorptivity, and, in the case of screening, by the absorption coefficient of the plume α_g. In the screening region ablated depth increases logarithmicaly with fluence and its qualitative behavior is weakly affected by the temperature dependence in α_g (T).

Small vaporization enthalpy results in a sub-linear $h(\phi)$ dependence, which, nevertheless, remains faster than logarithmic. With weakly absorbing materials ablation may proceed in two significantly different regimes -- without or with ablation of the heated subsurface layer. The latter occurs at higher fluences and reveals significantly higher ablation temperatures, but is weakly reflected on the ablation curves.

Calculations are performed in order to study the:
- influence of the duration and temporal profile of the laser pulse on the threshold fluence, ϕ_{th}. This is particularly important for strong absorbers were the heat conduction determines the temperature distribution.
- influence of the temperature dependences in material parameters on the ablation curves (ablated depth versus laser fluence) for regimes $\phi \approx \phi_{th}$ and $\phi >> \phi_{th}$.
- consequences of shielding of the incoming radiation at high fluences.
- differences in ablation curves for materials with big and small ablation enthalpy (e.g., metals and polymers which ablate thermally).

Nanosecond laser ablation has been studied for a large variety of different materials and laser wavelengths. As an illustrative example, the method is applied to the quantitative analysis of the single pulse ablation of polyimide Kapton™ H.

Keywords: laser ablation; thermal evaporation; analytical modeling, thermal ablation of polyimide

1. INTRODUCTION

Laser ablation is used in many technological applications in micropatterning and microfabrication, in the formation of thin films by pulsed-laser deposition, the formation of nanoclusters, etc. [1-3] . The fundamental interaction mechanisms involved in the ablation process have been described in [1] . One of the first questions which should be clarified by the theoretical analysis, is whether the experimental data can be explained on the basis of purely thermal surface evaporation, or other mechanisms (photochemical bond breaking, hydrodynamics, non-equilibrium excitation of electrons, multi-photon or saturation processes) play an important role.

The present paper deals with *purely thermal* ablation. At present, there exists a gap between a simple analysis based on the solution of the linear heat equation and the extensive numerical simulations performed on powerful computers. An effective feedback between the experimental and theoretical investigations requires a technique, that permits a rapid *quantitative* analysis of data by means of a PC. While with the ns ablation of metals the dominant role of thermal processes is widely accepted [2, 4] , in the field of polymer ablation the lack of quantitative analysis of experimental data on the basis of the purely thermal model in the broad range of parameters lead to many speculations and discussions [3, 5] . For polymers three quantities -- absorption length, thermal length and ablated depth may be comparable in a typical experiment. It has been realized, that this does not allow to use an approximation of surface absorption, or to neglect heat conduction [6, 7] or the movement of the ablation front [8]. Besides, activation temperature and enthalpy of vaporization may be significantly lower than with metals [9]. This makes temperature dependences of specific heat and thermal conductivity more important, which further complicates theoretical analysis[10] .

A powerful method to come around these difficulties seems to be the non-stationary averaging technique (moments technique, see e.g.,[11]) which provides a good approximate solution to the *nonlinear* heat equation. Here, one can take into account:

- arbitrary *temperature dependences* of material parameters, such as the specific heat, thermal conductivity, absorptivity, absorption coefficient, etc.
- arbitrary *temporal profiles* of the laser pulse;
- strong (Arrhenius-type) dependence of the ablation velocity on the surface temperature;
- *screening* of the incoming radiation by ablated product species;
- influence of the ablation (vaporization) enthalpy;
- influence of melting and/or other phase transformations.

Not included are hydrodynamical effects, nonlinear optical effects, optical breakdown, and thermally induced stresses.

In this paper we use this technique (which permits one to test the consequences of different assumptions very fast) to answer the following question. How do different factors influence the qualitative behavior of the ablation curves -- threshold fluence, the slope of the ablation curves, the decrease in slope at elevated fluences *within the frame of a purely thermal model.*

Nanosecond laser ablation has been studied for a large variety of different materials and laser wavelengths [1 - 8]. As an illustrative example, the method is applied to the quantitative analysis of the single pulse ablation of polyimide Kapton™ H. The single set of surface vaporization parameters (with activation energy 1.55 eV) describes satisfactory the ns-laser ablation at different wavelengths (248, 308 and 351 nm).

2. THE MODEL

For the analysis of thermal laser ablation one should solve the *nonstationary* heat conduction problem with ablation velocity $v = v(t)$ changing during the laser pulse. It is convenient to consider the thermal problem in terms of volumetric enthalpy H:

$$H(T) = \rho \int_{T_0}^{T} c(T_1)\, dT_1 \ , \tag{2.1}$$

where c is the specific heat (per unit mass) of the condensed phase, and T_0 the ambient temperature. The density of condensed phase ρ assumed to be constant. One-dimensional heat equation in the moving reference frame fixed with the ablation front reads [1]:

$$\frac{\partial H}{\partial t} = v\frac{\partial H}{\partial z} + \frac{\partial}{\partial z}\left(K\frac{\partial T}{\partial z}\right) + I_s\,\alpha\,\exp(-\alpha\, z) \equiv B(z,t), \tag{2.2}$$

where we introduced the notation B for the r.h.s. The heat conductivity K and the source term may depend on temperature T. Latent heat of phase transformations (e.g., melting) can be included into (2.1) by steplike increase in the enthalpy H near the melting point T_m. . The intensity within the solid shall obey Bouguer-Beer equation, with changes $\alpha\ z \rightarrow \int_0^z \alpha\,(z')\, dz'$ in the source term, if the absorption coefficient $\alpha \neq const.$ I_s is the (time dependent) intensity absorbed at the surface. Henceforth index "s" will refer to the quantities at the surface $z = 0$. In this work we adopt the following approximations. Following [4, 12-16], we relate I_s to laser pulse intensity $I(t)$ by

$$I_s = I\,A\,\exp\left[-\alpha_g\, h\right], \tag{2.3}$$

where A is the absorptivity, and α_g vapor absorption coefficient recalculated to the density of solid. Both may depend on T_s. The exponential term describes the shielding of radiation when thickness h of the solid material is ablated. The surface evaporation (ablation) rate v shall be given by [1, 4]:

$$v = v_0 \exp(-T_a / T_s), \tag{2.4}$$

where T_a is the activation temperature (in Kelvin), and v_0 is of the order of sound velocity. The heat equation (2.2) should be solved together with the boundary conditions. At the surface $z = 0$ one usually has *negative* thermal flux J_s [4, 9, 12]:

$$-K\frac{\partial T}{\partial z}\Big|_{z=0} = -v\left[L + H_g(T_s) - H(T_s)\right] \overset{def}{\equiv} J_s, \tag{2.5a}$$

The expression in square brackets is the enthalpy difference between the vapor and condensed phase at $T=T_s$. , L is the latent heat of vaporization per unit volume at $T_s = T_0$, and $H_g(T) = \rho \int_{T_0}^{T} c_g(T_1) dT_1$ is the enthalpy of vapor per unit volume of the condensed phase. c_g is the specific heat per unit mass of vapor phase at constant pressure (taken along the saturated pressure curve $p_{sat}\ (T)$). Approximations (2.4) and (2.5a) are valid significantly below the critical temperature

T_{cr}. . With $T_s \to T_{c\,r}$ $v(T_s)$ does not exceed sound velocity, and J_s (T_s) becomes determined by the kinetic energy of the expanding vapor and heat conduction in the (quite dense) gas phase. More refined approximations for $v(T_s)$ and J_s (T_s) can be derived from the equation of state and the processes in the Knudsen layer [4, 12].

From (2.5a) using (2.1) one can obtain the expression for the gradient of the enthalpy at the surface:

$$\left.\frac{\partial H}{\partial z}\right|_{z=0} = -J_s / D_s \quad \text{with} \qquad D_s \equiv K_s / \rho c_s \tag{2.5b}$$

where D_s is the thermal diffusivity at T_s. . The boundary condition at infinity $T(z\to\infty)\to T_0$ (and thus $H(z\to\infty) \to 0$) and initial condition $T(t=0) = T_0$ are obvious.

Though somewhat simplified [9, 12], this model is acceptable for the *quantitative* description of purely thermal surface laser ablation. It contains nonlinearities and nonstationary effects which can be analyzed numerically. This analysis requires big computational time [2, 17]. With the moment technique [11] which we will use in the further analysis, this problem can be reduced to three coupled nonlinear *ordinary* differential equations with a small loss in accuracy. These equations can be routinely solved by a fast algorithms included into many computational packages. Therefore, we obtain a convenient tool for the quantitative simulation of thermal effects in laser ablation.

3. MOMENTS METHOD

Here, we apply "moments method" or "nonstationary averaging" (see, e.g. [11]), for the analysis of laser ablation. The details of the procedure and the validation of the method's accuracy was discussed in [18].

The idea of the method is simple. The exact solution of the boundary value problem (2.1)-(2.5) fulfills (2.2) identically. If one uses some trial solution $H = H_p$ (z,t), the identity (2.2) will be violated. Nevertheless one can use H_p (z,t) as an *approximate* solution, if it obeys the "conservation laws" for the moments M_n :

$$\dot{M}_n = \int_0^\infty z^n B\left[H_p(z,t)\right] dz \ , \text{where } M_n = \int_0^\infty z^n H_p(z,t) dz \tag{3.1}$$

Here (2.2) was multiplied by z^n and integrated over z, and dot stands for differentiation with respect to time. This procedure warrants, that during the evolution of H_p (z,t) these conservation laws hold. As a result, the obtained set of equations has a clear physical sense. For example, the equation for M_0 reflects the *time-dependent* energy balance.

The number of differential equations in (3.1) should be equal to the number of time-dependent parameters characterizing H_p (z,t). We will consider two such parameters -- surface temperature T_s (t) and characteristic "thermal length" $l(t)$ for the enthalpy distribution. According to (3.1) we consider first *two* moments of *enthalpy* distribution. Equations (3.1), with the help of boundary condition (2.5a) yield:

$$\dot{M}_0 = -vH_s + J_s + I_s \equiv -v(L + H_{gs}) + I_s \tag{3.2a}$$

$$\dot{M}_1 = -v\ M_0 + \int_{T_0}^{T_s} K(T)\, dT + I_s / \alpha \tag{3.2b}$$

Here $H_s \equiv H(T_s)$, $H_{gs} \equiv H_g(T_s)$. We set the trial solution $H_p(z,t)$, in the form:

$$H_p(z,t) = \left[(H_s - \ell J_s / D_s)\, e^{-\alpha z} - (\alpha \ell H_s - \ell J_s / D_s)\, e^{-z/\ell}\right] / (1 - \alpha \ell) \tag{3.3}$$

This form satisfies obvious requirement $H_p(z=0,t) \equiv H_s(t)$ and boundary condition (2.5b). The first term in (3.3) describes the change of the enthalpy distribution with characteristic scale related to absorption of radiation, while the second term describes the changes related to heat conduction. It can be shown, that this function can approximate the solutions of heat equation in a broad range of parameters [18]. For example, with $\ell = 0$ it gives calorimetric solution. With $v = const.$ it coincides with the two-exponent solution of heat equation in the stationary ablation wave [4, 12], etc. Function (3.3) yields for the first two moments defined in (3.1):

$$M_0 = \left(\ell + \alpha^{-1}\right) H_s - \alpha^{-1} \ell J_s / D_s,$$

$$M_1 = \left(\ell^2 + \ell\alpha^{-1} + \alpha^{-2}\right) H_s - \left(\ell + \alpha^{-1}\right) \alpha^{-1} \ell J_s / D_s. \tag{3.4}$$

When (3.4) is substituted into (3.2), one obtains two ordinary differential equations for T_s and ℓ. Note, that all quantities should be finally written in terms of the surface temperature T_s. . Namely, one should insert J_s and D_s, from (2.5a), I_s and v from (2.3) and (2.4), as well as H_s from (2.1). It is not necessary to resolve the resulting equations with respect to dT_s/dt and $d\ell/dt$ for the numerical computations which have been done with the "*Mathematica*" software package [19].

The third equation for the thickness of ablated material (which is *coupled* to (3.2) via screening effect (2.3)) is given by

$$\dot{h} = v \overset{(2.4)}{=} v_0 \exp(-T_a / T_s) \tag{3.5}$$

Thus, the initial problem (2.1)-(2.5) is reduced to three *ordinary* differential equations for T_s, ℓ, and h which should be solved with the initial conditions

$$T_s(t=0) = T_0, \quad \ell(t=0) = 0, \quad h(t=0) = 0 \tag{3.6}$$

The study [18] shows, that their solution coincides with known analytical and numerical solutions of the initial problem (2.2)-(2.5) within 10%. It describes well the influence of the temperature dependent $c(T)$, $K(T)$ and $A(T)$ and, to a lower extent, $\alpha(T)$.

4. APPROXIMATE ANALYTICAL FORMULAS FOR THE GENERIC CASE

In this section we describe the most general features of ablation curves (ablated depth vs. fluence). The deviations from these dependences will be discussed in subsequent sections.

The temporal profile of the excimer laser pulse is approximated by the smooth function [1]

$$I(t) = I_0 \frac{t}{\tau} \exp\left[-\frac{t}{\tau}\right], \tag{4.1}$$

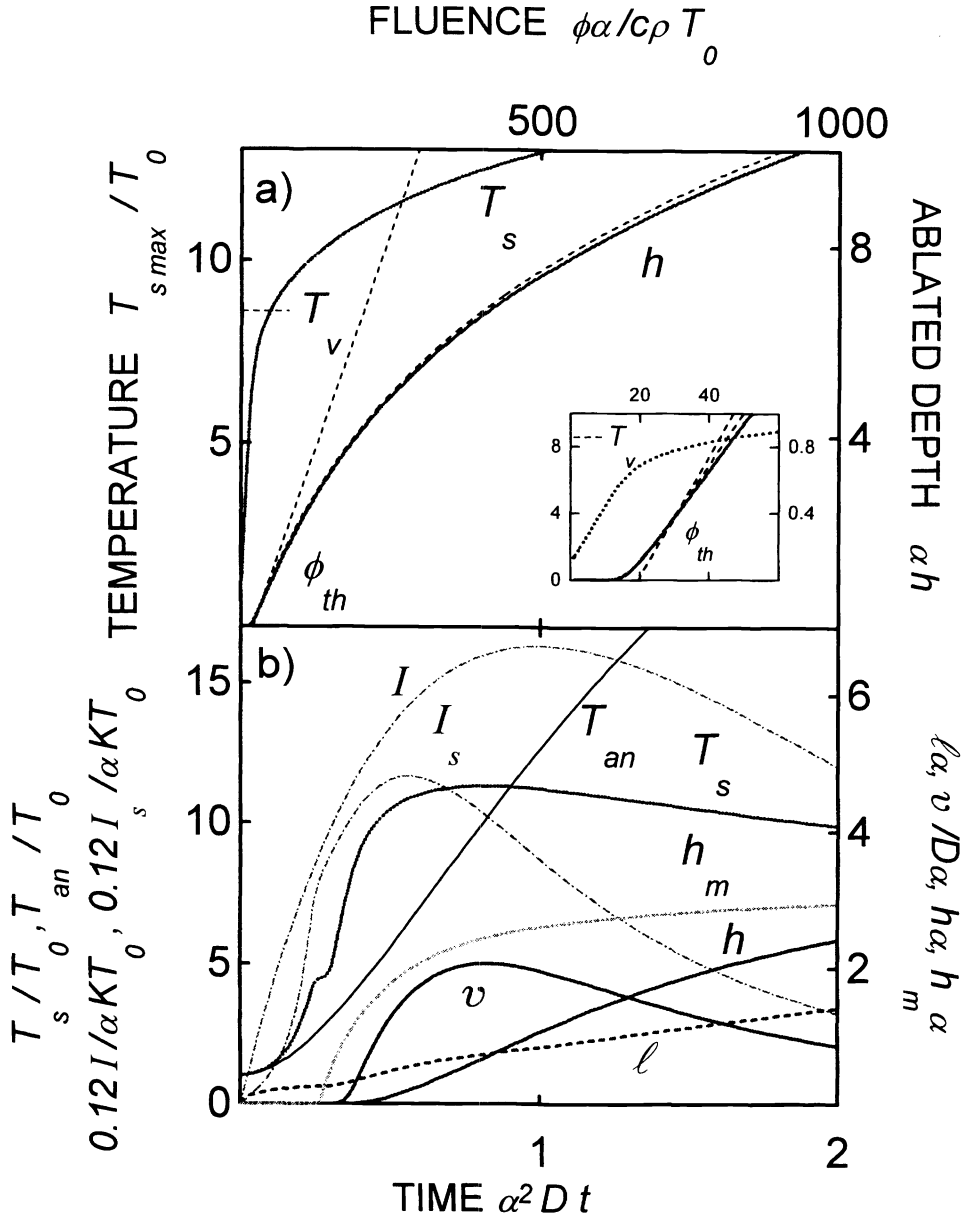

Fig. 1. a) Calculated dependence of ablated depth and maximum surface temperature on laser fluence. Smooth laser pulse (4.1). No melting. Dimensionless variables: Time $\alpha^2 Dt$, thermal length and ablated depth $\alpha\ell$, αh, velocity $v/\alpha D$, temperature T_s/T_0, intensity $I/\alpha K T_0$, fluence $\phi\alpha/c\rho T_0$. Constant parameters satisfy the following conditions: $A = 1$, $\alpha^2 D\tau = 1$, $v_0/D\alpha = 10^3$, $L/\rho c T_0 = 20$, $T_a/T_0 = 70$, $H_g = H$, $\alpha_g = 0.2\alpha$. These combinations arise in dimensionalization of equations. They correspond, e.g., to $\tau = 10$ ns, $D = 10^{-2}$ cm^2/s, $\alpha = 10^5$ cm^{-1}, $v_0 = 10^6$ cm/s, $T_a = 21000$ K $\equiv 1.81$ eV, $T_0 = 300$ K, $c = 1$ J/g K, $\rho = 1$ g/cm^3, $L = 6$ kJ/cm^3, which are typical numbers for strongly absorbing polymers. For these numbers, unit of dimensionless time, is 10 ns, of temperature 300 K, spatial unit 0.1 μm, and unit of fluence 3 mJ. Ablated depth per pulse (solid curve) and maximal surface temperature (dotted curve) are calculated from the nonstationary moments approximation (3.2), (3.5). Here, and *in subsequent figures, thin dashed lines* show linear approximation (4.5), and/or logarithmic approximation (4.12). Inset shows near threshold behavior.

b) Time evolution of the surface temperature (dotted curve), ablated depth and ablation velocity (solid curves), thermal length (dashed curve) and molten depth (dash-double dot). Temporal shape of laser pulse and the laser intensity at the surface are shown by dash-dotted, and temperature calculated analytically neglecting melting and ablation by thin solid curve. $\phi\alpha/c\rho T_0 = 370$. $\alpha_g = 0.5\alpha$, and melting $T_m/T_0 = 4.5$, with the latent heat of fusion $H_m/\rho c T_0 = 3$ is introduced. Absorptivity increases linearly from $A(T_\infty) = 0.2$ to $A(T_s \geq T_m) = const = 0.9$. $K(T > T_m) = 3K$ $(T < T_m)$. Other parameters as in Fig. 1a.

The laser fluence is given by $\phi = I_0\tau$ and the duration of the pulse at the full widths at half maximum $t_{FWHM} \approx 2.446\tau$ and $t_\phi \equiv \phi / I_{max} \approx 2.718\tau$. The analytical solution of the linear heat equation $T_{an}(t)$ presented for comparison is given by [1]:

$$T_{an}(t) = T_0 + \frac{\alpha}{\rho c}\int_0^t I(t-t_1)\exp\left[\alpha^2 D t_1\right] erfc\sqrt{\alpha^2 D t_1}\, dt_1 , \qquad (4.2)$$

where parameters of the material are taken at $T = T_0$.

Figure 1 (solid line) gives an example of calculated ablation curve, which corresponds to the case which we call "generic". Heat penetration depth ~ $(D\tau)^{1/2}$, absorption length α^{-1} and ablated depth h are all comparable in this region. This does not allow to neglect heat conduction, or energy spent on ablation as it is done in some of the models [7, 20, 21]. The example of such a system can be ns excimer-laser ablation of polymers strongly absorbing in the UV. The values of parameters and the meaning of dimensionless quantities is given in the caption to the Fig. 1. Despite the relative complexity of the time-dependent thermal ablation problem formulated in section 2, the ablation curve demonstrates remarkable simplicity. This simplicity holds in the broad range of material parameters, even if some of them depend significantly on temperature. One can subdivide the ablation curve into three regions (see figure): Arrhenius tails, linear region and screening region. We discuss them separately.

Linear region and the ablation threshold.

At moderate fluences, the ablation curve in Fig. 1 demonstrates linear increase of h with fluence. If screening can be neglected, linear increase continues up to very high fluences. This behavior is not self evident, taking into account possible temperature dependences in material parameters and essential non-stationarity of the process (see Fig. 2). The common argument is that one can consider an ablation process quasi-stationary, with the velocity at each moment of time determined by the corresponding intensity [22]. This is not quite true for ns laser pulses. Even for the constant intensity, the time to reach stationary regime is estimated as [4, 12]:

$$t > \max(1/\alpha v,\quad CD/v^2)\,,\ C \approx 8 \qquad (4.3)$$

The second condition is certainly wrong for Figs. 1,2, and it is even less fulfilled e.g., for metals in ns pulses. From Fig. 2 one can see, that the thermal length ℓ by no means stabilizes during the pulse. Neither does it correlate with the intensity $I(t)$, as it would have been for the quasi-stationary ablation. In fact, even at fluences $\phi \approx 2\div5\ \phi_{th}$ (depending on particular numbers), ℓ is almost unaffected by the ablation. That means that it is *wrong* to solve stationary or quasi-stationary heat conduction equation *within* the material during the pulse. The *surface* temperature behaves quasi-stationary, but *inside* the material this may be completely untrue. The heated volume increases during all the duration of the pulse. Nevertheless, the $h(\phi)$ dependence *is* indeed linear usually above $2\div3\phi_{th}$, as predicted by the quasi-stationary consideration, though for somewhat different reasons. These reasons are: conservation of energy and sharp $v(T)$ dependence. The latter leads to the fact, that during ablation $v(t)$ changes with time much faster than $T_s(t)$ (see Fig. 2). This is not necessarily true with respect to $\ell(t)$! (see in Fig. 1b)..

Having this in mind, we integrate (3.2a) over time up to the moment when both ablation and laser irradiation are finished. $L+H_{gs}$ is a smooth function of T_s, and can be considered as constants in comparison to v. We also assume constant absorptivity A in this section. This, together with (3.4) for the M_0, when ablation is already finished and $v = 0$, and $J_s = 0$, yields:

$$A\phi = h(L + H_{gs}) + H_s(\ell + \alpha^{-1}) \tag{4.4}$$

This reflects the overall energy conservation law. Absorbed laser fluence is spent on ablation (first term in the r.h.s.) and heating of the bulk (second term, which represents moment M_0). Note, that at big times, when $I = 0$, $v = 0$; moment M_0 stays constant (see (3.2a)), and enthalpy is only redistributed within the material as H_s decreases and ℓ increases. It turns out, that in rather broad range of parameters above threshold second term in (4.4) weakly depends on fluence. Thus (4.4) yields linear $h(\phi)$ dependence. Below we formulate several rules of thumb which allow to find the parameters of this dependence.

At low fluences, the last term in r.h.s. of (4.4) dominates - the fluence is spent predominantly on the heating of

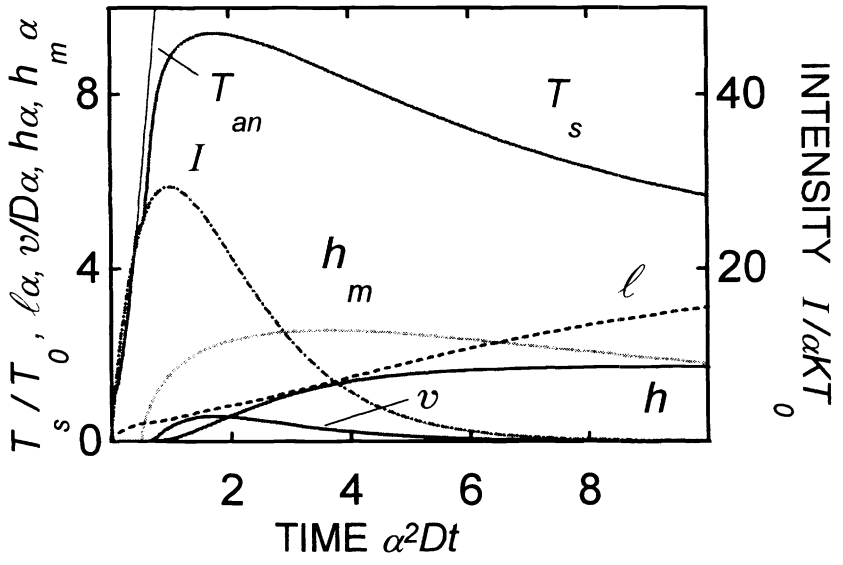

Fig. 2. Calculated time evolution of the surface temperature (dotted curve), ablated depth and ablation velocity (solid curves), thermal length (dashed curve) and molten depth (dash-double dot). Temporal shape of laser pulse is shown by dash-dotted, and temperature calculated analytically neglecting melting and ablation by thin solid curve. Dimensionless fluence $\phi\alpha/c\rho T_0 = 80$. No screening, $\alpha_g = 0$, and melting $T_m/T_0 = 5$, with the latent heat of fusion $H_m/\rho cT_0 = 2$ is introduced. Other parameters and meaning of dimensionless quantities are the same as for Fig. 1.

material. In this region T_s and H_s at the end of the pulse depend significantly on fluence. This is Arrhenius region, which depends strongly on temperature dependences in material parameters and will be discussed later.

With higher fluences the first term in r.h.s. of (4.4) dominates. This is the linear regime, where

$$h \approx B(\phi - \phi_{th}) \ , \ B = \frac{A}{(L + H_{gs})} \ , \ \phi_{th} = \frac{H_s(\ell + \alpha^{-1})}{A} \tag{4.5}$$

Quantities which determine B and ϕ_{th} may depend on temperature. Due to strong $v(T_s)$ dependence T_s does not change significantly during the ablation regime. From this point of view one can take the values of all quantities, say, at boiling temperature T_b. Nevertheless, this choice is too arbitrary. We define the vaporization temperature T_v as the temperature, where the transition from the Arrhenius to linear regime occurs in the $h(\phi)$ dependence.

This happens when two terms in (4.4) are comparable, i.e., laser energy splits equally between the vaporization and the heating of material. We approximate h and ℓ near the threshold as:

$$h \approx v(T_v)\, t_{FWHM}\ ,\ \ell \approx (\langle D(T_v)\rangle\, t_{FWHM})^{1/2}\ ,\ \text{with}\ \langle D(T_v)\rangle \equiv \left[\int_{T_0}^{T_v} K(T)dT\right] / H(T_v) \tag{4.6}$$

and equate both terms in r.h.s. of (4.4). This yields the equation for T_v :

$$v(T_v)\, t_{FWHM}\left[L + H_g(T_v)\right] = H(T_v)\left[(\langle D(T_v)\rangle\, t_{FWHM})^{1/2} + \alpha^{-1}\right] \tag{4.7}$$

In order to illustrate the meaning of the average diffusivity $<D>$ in (4.6)-(4.7), let us introduce

$$M = \alpha\ M_1 - M_0 \equiv H_s \ell^2 \alpha - \ell^2 J_s / D_s \tag{4.8}$$

Then, using (3.2) one obtains:

$$\dot{M} = \alpha \int_{T_0}^{T_s} K(T)dT - v\, M/\ell - J_s \tag{4.9}$$

Interestingly, (4.9) does not depend on intensity (even if the screening is present) and reflects the influence of heat conduction on the enthalpy distribution within the solid. If we assume that velocity related terms are small (i.e., $v = 0$, $J_s = 0$) and assume $T_s \approx T_v$ during the time t_{FWHM}, which is significantly longer than the initial stage of heating, (4.9) leads to (4.6). This consideration does not *prove* the expression for ℓ and the averaging adopted for the diffusivity in (4.6). Equations (4.6)-(4.7) for T_v should be considered as a rule of thumb. Their validity was confirmed by comparison with the numerical solution of (3.2) with different temperature dependences in $K(T)$ and $c(T)$, and for different laser pulse shapes. If the t_ϕ is used instead of t_{FWHM}, the results are similar. Linear dependence (4.5), calculated with (4.7) for T_v is shown in Fig. 1 by the dashed line. The values of T_v and ϕ_{th} are given in the figure caption.

In a more refined approach, one can integrate (4.9) in a way similar to that which resulted in (4.4), and solve resulting equations with respect to ℓ and h simultaneously. However, this is complicated by the necessity to integrate expressions like $\ell\, dh$, because ℓ may change as fast as h. Approximations which allow to obtain compact result are too crude and smear out some qualitative effects, which will be discussed below. The important feature is that with good heat conductors ($\alpha^2 D\tau >> 1$) the transition to the linear regime is sharper, and the linear law (4.5) is fulfilled in the wider range of parameters.

Several comments on the linear dependence (4.5) are appropriate.

i) Threshold fluence should be defined from the linear (or logarithmic, see below) part of the ablation curves. Definitions based on the measurements in the Arrhenius tails depend strongly on the sensitivity of measuring devices.

ii) Changes in low temperature behavior of material parameters do change ϕ_{th}, but not the slope B of the ablation curve.

iii) With $\phi >> \phi_{th}$ ablation curves are quite insensitive to the temperature dependences of material parameters. The slope B depends only on high temperature value of absorptivity and vaporization enthalpy.

iv) The threshold fluence ϕ_{th}, as defined by (4.5) is *not* the fluence "spent on heating before the ablation starts". It is what is ultimately wasted on heating, when the ablation *is finished.* The heating of the bulk of material takes place also *during* the ablation.

The last notion explains, why good heat conductors better obey linear law (4.5). The heat losses in this case are independent of ablation even at relatively high fluences. Therefore, the opinion that the heat conduction diminishes the slope of ablation curves at high fluences, due to "decrease of threshold fluence with intensity" [22] is wrong. Even if at low fluences heating losses are higher, the heated region is more extended in this case and cools slower. This leads to a stronger ablation after the pulse, which results in smooth behavior of ablation curves.

Screening region

Following [4, 8, 12 - 15, 22], we adopted the expression for screening (2.3), which considers the optical thickness of the plume to be proportional to the current value of h. With this assumption we can multiply (3.2a) by $A^{-1}\exp(\alpha_g h)$ and rewrite it in a differential form:

$$d\phi = A^{-1}(L + H_{gs})\mathrm{e}^{\alpha_g h}\, dh + A^{-1}\mathrm{e}^{\alpha_g h}\, dM_0 \tag{4.10}$$

Now we integrate (4.10), with the argumentation similar to that which lead to (4.4). In the first term in r.h.s. all T_s-dependent quantities are slow when $dh = vdt \neq 0$, and their values at T_v defined by (4.7) should be taken. The second term is more complicated. M_0 (which represents the losses to heating of the condensed phase) changes only when ablation is present ($v \neq 0$) or radiation reaches the surface ($I_s \neq 0$) (see (3.2a)). This is fulfilled as long as $\alpha_g h < 1$, $\exp(\alpha_g h) \approx 1$. If we assume that screening does not significantly shorten the duration of laser intensity which reaches the surface, we have for the last term in (4.10):

$$A^{-1}\int \exp(\alpha_g h)\, dM_0 \approx A^{-1} M_0(t_{FWHM}) \equiv \phi_{th} \tag{4.11}$$

The last identity follows from (3.4), (4.5). With this approximation, (4.10) yields for h after the integration

$$h = \frac{1}{\alpha_g}\ln\left[1 + \alpha_g B(\phi - \phi_{th})\right] \tag{4.12}$$

with B and ϕ_{th} given by (4.5) as before. The dependence (4.12) is shown in Fig. 1 by the thin dashed curve. Similar result was obtained in [22] from the quasi-stationary wave approximation. At moderate fluences, i.e., with $\alpha_g h << 1$, (4.12) coincides with no screening result (4.5). This: i) justifies the approximation (4.11) in this region; ii) allows to determine ϕ_{th} from the logarithmic fit to the ablation curves, as well as from the linear one.

With higher fluences $\alpha_g h >> 1$, which leads to:

i) Shortening of the effective laser pulse of the surface (Fig. 3). This *decreases* the losses on heating of the material (M_0 in (4.11) gets smaller due to the decrease in ℓ at the end of the ablation process.

ii) The factor $\exp(\alpha_g h)$ in (4.11) *increases*.

As a result of competition between these two factors, (4.12) holds in quite broad range of parameters. With $\phi >> \phi_{th}$ the exact value of energy spent on heating of the specimen (ϕ_{th} term) is unimportant anyway.

5. ARRHENIUS TAILS

Approximations (4.5), (4.12) predict, that *well above* the threshold the slope of ablation curves is rather *insensitive* to specific heat and thermal conductivity of the material. In this section we study how these parameters and the temporal shape of the laser pulse influence *near threshold* ablation and ϕ_{th} itself.

Clearly, in this region no simple approximations exist. Suffice it to recall, that time-dependent heat equation with temperature dependent parameters does not have an analytical solution even when ablation is absent. To find an ablated depth per pulse h, one has to take into account surface recession and to calculate an integral

$$h = \int_0^\infty v_0 \exp\left[-T_a / T_s(t)\right] dt \tag{5.1}$$

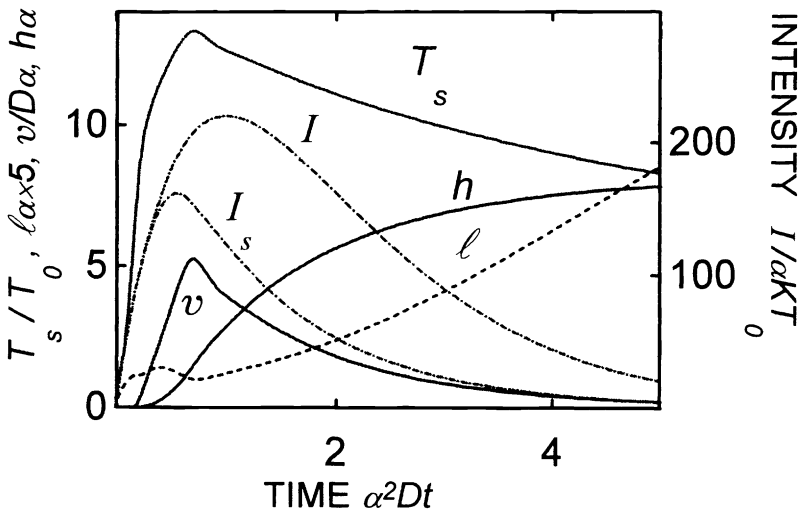

Fig. 3. Time evolution of the surface temperature (dotted curve), ablated depth and ablation velocity (solid curves), and thermal length (dashed curve). Temporal shape of laser pulse and the intensity which reaches the surface I_s, are shown by dash-dotted curves. Dimensionless fluence $\phi\alpha/c\rho T_0$ = 600. All parameters and meaning of dimensionless quantities are the same as for Fig. 1.

Method of moments yields both the estimation for the T_s *(t)* dependence with temperature dependent parameters and non-zero surface velocity, and automatically calculates ablated depth h via (3.5). The time necessary to solve differential equations (3.2), (3.5) is in fact *shorter* than that required for the numerical integration (5.1) with known T_s *(t)* dependence.

Specific heat

Specific heat usually increases with T and well above the Debye temperature follows the Dulong - Petit law [9, 23, 24]:

$$c_\infty = 3Rm/\mu \tag{5.2}$$

Here, R is the gas constant, m the number of atoms in a structural unit, μ the molar weight. While with metals, c usually stabilizes at $T<<T_v$, with polymers it is often not the case [9]. We adopted the following approximation:

$$c(T) = c_\infty + (c_0 - c_\infty)\exp\left[(T_0 - T)/\ T_c\right] \tag{5.3}$$

The meaning of coefficients is clear: c_0 is the specific heat at T_0 and T_c determines how fast does c approach c_∞. Figure 4 shows, how *c(T)* dependence influences near threshold ablation. Screening is neglected. One can see, that *c(T)* dependence only shifts ϕ_{th}. This is reflected also by the approximation (4.5)-(4.7) (thin dashed lines). The slope B is almost unaffected. With increasing c_∞, the slope somewhat decreases due to increase in H_{gs} in (4.5). Note, that we assumed $H_{gs} \equiv H_s$, (high molecular weight of the ablation products). But even with monatomic evaporation, under the simplest assumption $c=3R/\mu$, c_g = $5R/2\mu$, the difference between H_{gs} and H_s. is quite small in comparison to L in (2.5a). Arrhenius inset (log(h) vs.

reciprocal fluence) reveals influence of $c(T)$ dependence, and some deviations from the linear behavior. Threshold fluences and vaporization temperature T_v, estimated from (4.5)-(4.7) are listed in the figure caption.

Thermal conductivity

For the $K(T)$ dependence we used a power function [1]:

$$K(T)=K_0(T/T_0)^n \tag{5.4}$$

As expected from the approximations (4.5)-(4.7), $K(T)$ dependence almost does not influence the slope B of the ablation curves. The small differences which exist are due to the difference in T_v and, correspondingly H_g (T_v). This is confirmed by Fig. 5. For the numbers used for this figure, the decrease in K has less pronounced effect, than the increase in K with temperature. This is because with smaller K, $\alpha^2 D\tau < 1$ with these numbers and we are in a "calorimetric region", where $K(T)$ dependence is unimportant. Increase in K makes $\alpha^2 D\tau > 1$. With this condition the initial heating is mainly determined by

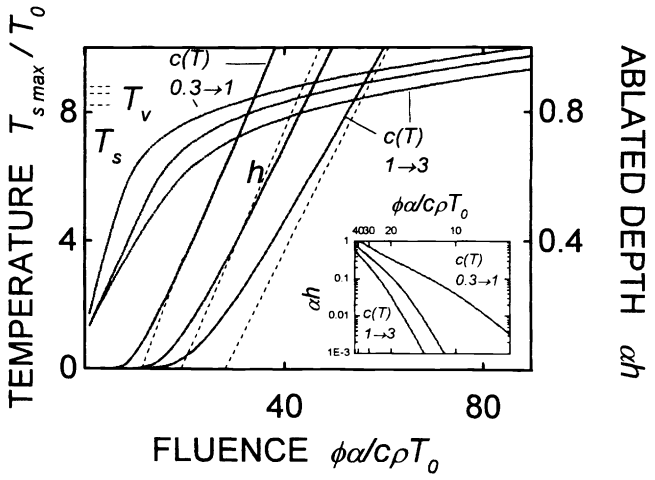

Fig. 4. The influence of the temperature dependence in specific heat $c(T)$ given by (5.3) onto ablation curves (solid) and maximum temperature (dotted) curves. Thin dashed lines present linear approximations (4.5). Upper curves c_0 =0.3, c_∞ =1, $\phi_{th}\,\alpha/c\rho T_0$ = 11.6, T_v/T_0 = 8.22; Lower curves c_0 = 1, c_∞ = 3, $\phi_{th}\,\alpha/c\rho T_0$ = 27.9, T_v/T_0 = 8.8; T_c = 10 in both cases. Central curves: c=1, $\phi_{th}\,\alpha/c\rho T_0$ =19.5, T_v/T_0 = 8.59. No screening, α_g =0. Other parameters are the same as for Fig. 1. Inset shows Arrhenius plots: ablated depth (logarithmic scale) vs. fluence (reciprocal scale).

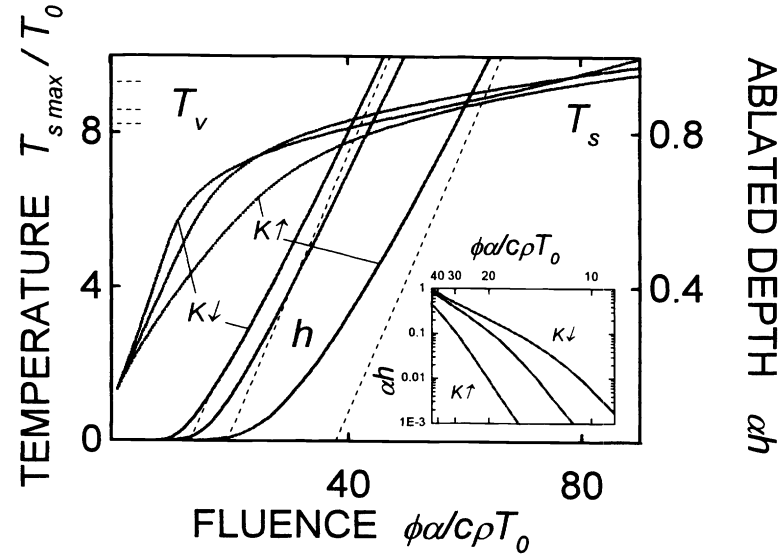

Fig. 5. The influence of the temperature dependence in thermal conductivity $K(T)$ given by (5.4) onto ablation curves (solid curves) and maximum temperature (dotted curves). For the curves marked $K\downarrow$, n = -1, $\phi_{th}\,\alpha/c\rho T_0$ = 13.3, T_v/T_0 = 8.22; for the curves marked $K\uparrow$, n =1, $\phi_{th}\,\alpha/c\rho T_0$ = 37.9, T_v/T_0 = 9.32. Central curves correspond to n = 0, $\phi_{th}\,\alpha/c\rho T_0$ = 19.5, T_v/T_0 = 8.59. No screening, α_g = 0. Other parameters are the same as for Fig. 1. Inset shows Arrhenius plots: ablated depth (logarithmic scale) vs. fluence (reciprocal scale).

the heat conduction. Stronger heat conduction prolongs the transition to the linear regime. With higher values of K_0 in (5.4), if $\alpha^2 D_0 \tau >> 1$, decrease in K influences the ablation curve stronger, but still less than increase in K with the same power n.

In a certain fluence interval the $T_{s\,max}$ for decreasing $K(T)$ is lower than with K=const. This is because in this region the *maximum* velocity for the former is lower, which leads to *bigger* losses on heating of material. This however, does not reflect on the overall ablation curves due to the differences in the post-pulse ablation. This effect will be further discussed in section 6.

Vaporization parameters

Figure 6 illustrates the influence of vaporization parameters on the ablation curves. One can see, that the activation temperature T_a and the preexponential factor v_0 only shift the ablation threshold, and this shift is reflected by the approximation (4.5)-(4.7). More important is the influence of the latent heat of sublimation L. A twofold decrease in L

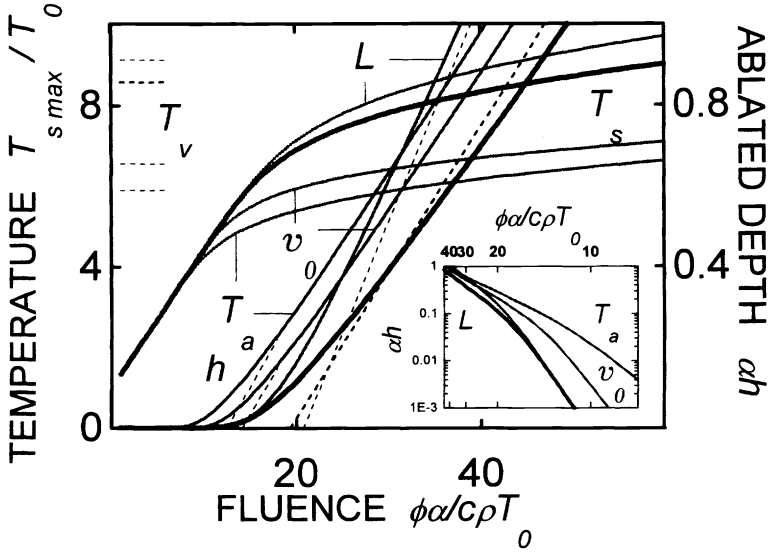

Fig. 6. The influence of the parameters of surface vaporization onto ablation curves (solid curves) and maximum temperature (dotted curves). The following examples are given: Activation temperature is decreased up to T_a/T_0 =50 ($\phi_{th}\alpha/c\rho T_0$ = 12.5, T_v/T_0 =5.89); preexponential factor is increased up to $v_0/D\alpha$ = 10^4, ($\phi_{th}\alpha/c\rho T_0$ = 14.2, T_v/T_0 =6.55); Ablation enthalpy is decreased up to $L/\rho c T_0$ =10, ($\phi_{th}\alpha/c\rho T_0$ =20.9, T_v/T_0 =9.14). No screening, α_g =0. Other parameters are the same as for Fig. 1, and corresponding curves ($\phi_{th}\alpha/c\rho T_0$ =19.5, T_v/T_0 =8.59) are shown for reference by the thicker curves. Inset shows Arrhenius plots: ablated depth (logarithmic scale) vs. fluence (reciprocal scale).

significantly increases slope B, and makes the transition to the linear regime less sharp. At the same time approximations (4.5)-(4.7) work worse, because with small L, the deviations of T_s from T_v play a more important role. The extreme case $L = 0$ is discussed below in connection with Fig. 9.

6. DEVIATIONS FROM THE GENERIC CASE

In the previous section we considered the cases, where simple formulas (4.5)-(4.7) or (4.12) provide reasonable approximations to the ablation curves calculated from the moments approximation (3.2), (3.5). In this section we study several cases when these approximations do not reflect important peculiarities of the ablation process and/or etch curves. Having in mind that the calculations with the moment method are not much slower than with the analytical formulas, this will further demonstrate the convenience of the suggested approach.

Temporal profile of the laser pulse

Approximations (4.5)-(4.7) suggest, that laser pulses of different shapes with the same t_{FWHM} result in identical ablation curves. In the region $\alpha^2 Dt_{FWHM} >> 1$ where the losses to the heating of the specimen and ϕ_{th} are determined by the heat conduction, this is not the case. Correspondingly, approximations (4.6)-(4.7) become too crude in this region. Figure 7 illustrates the matters. Here, ablation by three pulses was calculated: smooth pulse (4.1), rectangular pulse, and symmetric triangular pulse. All pulses have the same t_{FWHM}. The values of parameters are listed in figure caption. Note a significant increase in dimensionless time in comparison to previous figures. One can see, that the ablation curve for the rectangular pulse *is not* close to that of the smooth pulse with the same t_{FWHM} . (In fact, for the numbers used, it follows quite closely the ablation curve for the twice shorter smooth pulse). While the solution of moments approximation reveals significant influence of the pulse shape onto ϕ_{th} (see Fig.), this by definition is *not reflected* by the approximation (4.5)-(4.7) or other approximations of this type. Figure 8 shows the evolution of the ablated depth and temperature for these three pulses at a near threshold fluence. With the fixed t_{FWHM} rectangular pulse results in the highest T_{max} due to the absence of "tails" which lead to higher heat losses.

The dependence of ablation curves on the shape of the pulse is important for comparison of the experimental results obtained by different groups. Besides, excimer lasers usually have sharper front edge and larger t_{FWHM} with higher overall energies of the pulse.

Small ablation enthalpy

In the case of polymers, ablation products may have much higher molecular weight than for simple inorganic materials [5, 28] . As a result, ablation enthalpy *per* cm^3 *or per gram of material* is significantly decreased, and the specific heat and enthalpy of the condensed and the gas phase are almost equal. Besides, polymers easier undergo thermal destruction [9]. An extreme case with $L = 0$ and low $T_a / T_0 = 40$ is considered in Fig. 9. The behavior of $T_{s\,max}$ is similar to the generic case, and one can notice ablation threshold associated with significant increase in $v(T_s)$. At the same time:

i) at low fluences the $h(\phi)$ dependence has an inflection point.

ii) at high fluences the $h(\phi)$ dependence is slower than linear. This decrease in slope has totally different origin than that which is due to the screening. Its parameters are determined by the $v(T_s)$ and $H_g(T_s)$ dependences and cannot be expressed by an analytical formula.

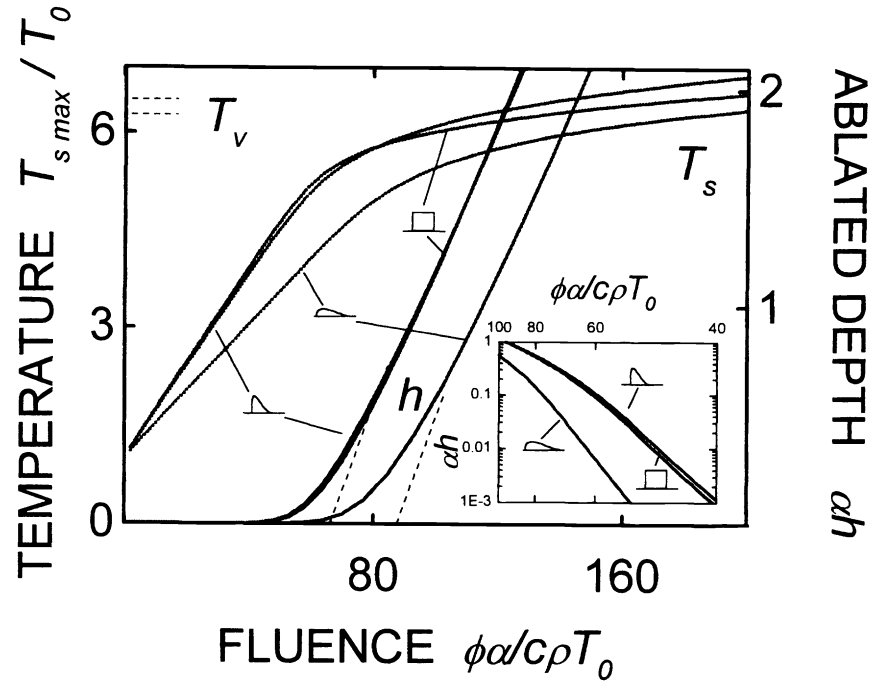

Fig. 7. The influence of the laser pulse shape onto ablation curves (solid curves) and maximum temperature (dotted curves). No screening, $\alpha_g = 0$. Three pulses are considered: smooth pulse (4.1) with $\alpha^2 D\tau = 100$ rectangular pulse, and symmetric triangular pulse. The increase in $\alpha^2 D \tau$ may correspond e.g., to $\alpha = 10^6$ cm^{-1}, $v_0 = 10^7$ cm/s, with the unit of dimensionless fluence 0.3 mJ, other parameters being the same as for Fig. 1. All pulses have the same t_{FWHM}: $\alpha^2 D\, t_{FWHM} = 244.6$ and, therefore equal $\phi_{th}\, \alpha /c\rho T_0 = 87.7$, $T_v /T_0 = 6.27$ calculated from (4.7). Small pictures in the plot indicate which curve refer to which pulse. Inset shows Arrhenius plots: ablated depth (logarithmic scale) vs. fluence (reciprocal scale).

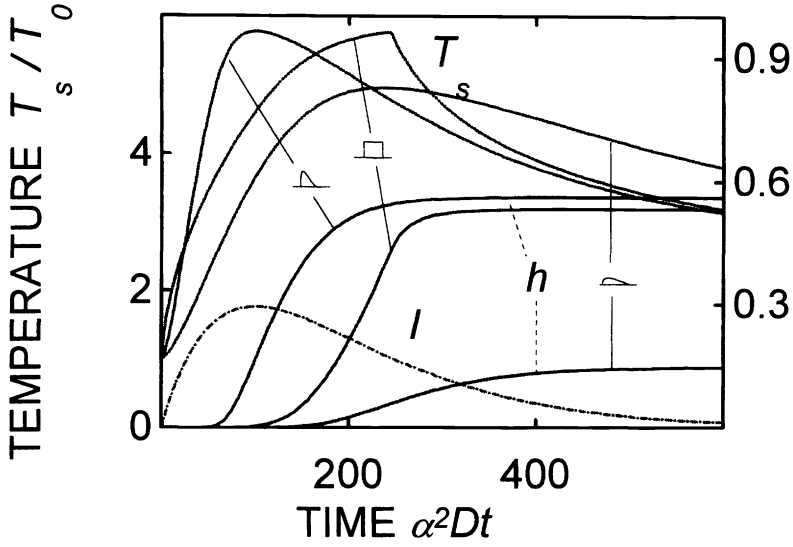

Fig. 8. Calculated time evolution of the surface temperature (dotted curve), and ablated depth (solid curves) for the pulses of different shapes (shown by dash-dotted curves) described in Fig 7. Dimensionless fluence $\phi\alpha /c\rho T_0 = 80$.

Temperature dependent shielding

At high fluences, with optical breakdown and plasma formation the amount of ablated material almost exclusively depends on the properties of the plume. In this region constant α_g approximation is too crude. To understand the general trends, we consider a model dependence

$$\alpha_g / \alpha = C \exp(-T_\alpha / T_s) \qquad (6.1)$$

which reflects very sharp growth of plasma absorption with temperature due to ionization (Kramers - Unsöld formula[12, 25,26]).

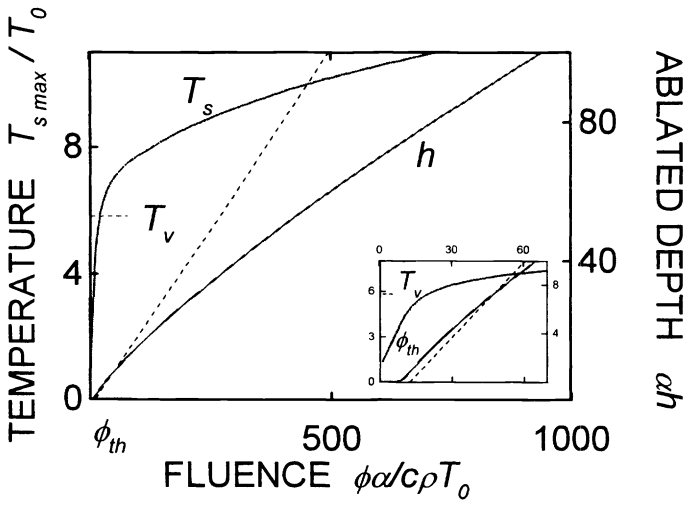

Fig. 9. The case of easily decomposing material with no ablation enthalpy: $T_a/T_0 = 40$, $L/\rho cT_0 = 0$, ($\phi_{th}\ \alpha/c\rho T_0 = 12.4$, $T_v/T_0 = 5.83$). No screening, $\alpha_g = 0$. Other parameters are the same as for Fig. 1. Ablation curves (solid) and maximum temperature (dotted) curves. Inset shows near threshold behavior. Ablated depth significantly deviates from the linear behavior.

The result of calculations is presented in Fig. 10. Despite sharp temperature dependence (6.1), the ablation curve resembles the generic case depicted in Fig. 1. At low fluences, it more closely follows linear approximation (4.5). At high fluences the $h(\phi)$ dependence is somewhat slower than logarithmic. The transition to the screening regime occurs at such fluences, where $\alpha_g\ (T_{s\,max})h(T_{s\,max}) \approx 1$, and at higher fluences is rather insensitive to the details of $\alpha_g\ (T_s)$ dependence.

More refined approach shall include consideration of the plasma heating via absorption of radiation and energy exchange between the plasma and the substrate. The consideration of the plasma also can be done on the basis of averaging procedure [16, 27]. This allows to avoid solution of partial differential equations altogether.

Ablation of weakly absorbing materials

An important situation in which the approximations (4.5)-(4.7) systematically fail, is the ablation under the condition $\alpha^2 D\tau << 1$ (e.g., weakly absorbing polymers [5, 28]). Here, for a certain values of parameters four stages of heating and ablation may be observed during the modeling of single pulse ablation (Fig. 11). Initially, heating proceeds calorimetricaly, that is both the surface movement and the heat conduction may be ignored. Then, surface velocity becomes

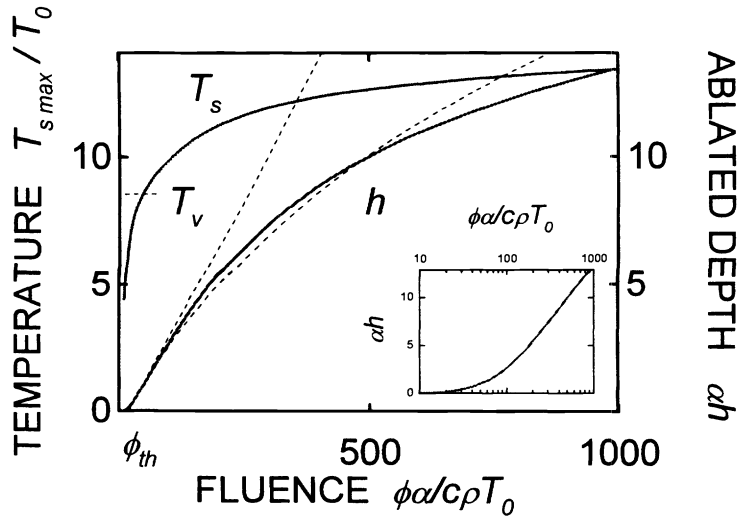

Fig. 10. Temperature dependent screening (6.1) with $T_\alpha = 130T_0$, $C = 10^4$. ($\alpha_g \approx \alpha$ with $T_s/T_0 \approx 14.1$). Other parameters are the same as for Fig. 1. ablation curves (solid) and maximum temperature (dotted) curves. Logarithmic approximation (4.12) (thin dashed curve) is calculated with $\alpha_g/\alpha = 0.1$. Inset shows ablated depth vs. logarithmic fluence.

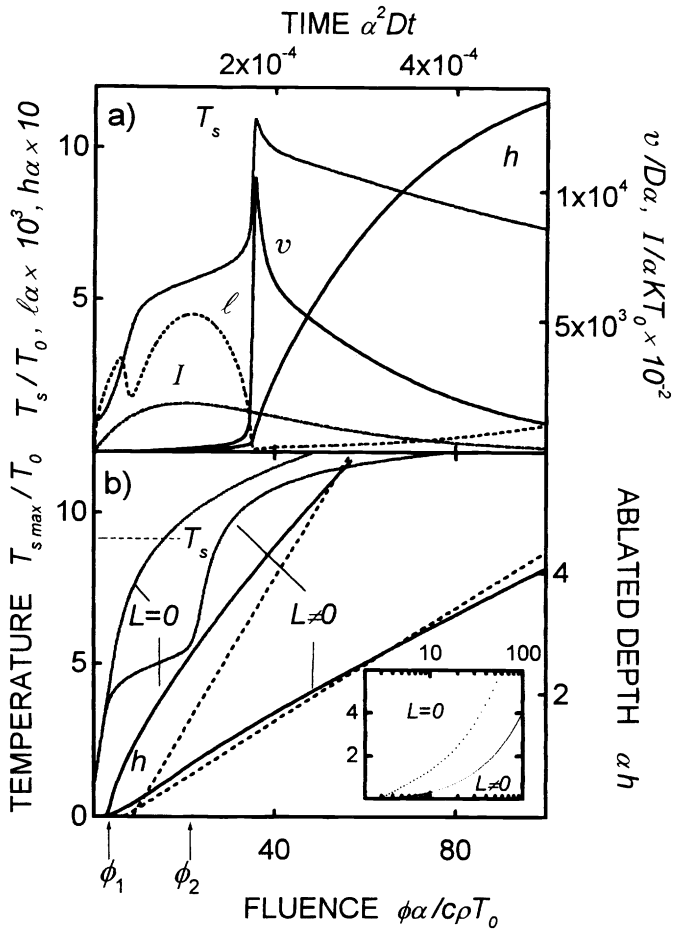

Fig. 11. a) Explosive ablation ("second threshold") in the heating of weakly absorbing materials. Time evolution of the surface temperature (dotted curve), ablated depth and ablation velocity (solid curves), and thermal length (dashed curve). Temporal shape of laser pulse is shown by dash-dotted curve. Dimensionless fluence $\phi\alpha/c\rho T_0$ =50. Constant parameters satisfy the following conditions: A=1, $\alpha^2 D\tau$=10^{-4}, $v_0/D\alpha$=10^6, $L/\rho cT_0$ =15, T_a/T_0 =50, $H_g = H_s$, α_g = 0. This corresponds, e.g., to τ =10 ns, D=10^{-3} cm^2/s, α = 3.16×10^3 cm^{-1}, v_0 = 3.16×10^6 cm/s, T_a = 15000 K ≡ 1.29 eV, T_0 =300 K, c =1 J/gK, ρ = 1 g/cm^3, L=4.5 kJ/cm^3, (ns UV-ablation of weakly absorbing polymers). For these numbers, unit of dimensionless time, is 100 μs, unit of temperature 300 K, unit of ablated depth or thermal length is 3.16 μm, and unit of normalized fluence is 95 mJ.

b) Ablation curves for weakly absorbing material with ($L/\rho cT_0$ =15) and without (L=0) "second threshold". Other parameters are the same as for a). $\phi_{th}\,\alpha/c\rho T_0$ =6.58, T_v/T_0 = 7.48. Second threshold (6.2) $\phi_2\,\alpha/c\rho T_0$ = 21.48, and threshold calculated from (6.5) $\phi_1\ \alpha/c\rho T_0$ =2.98, T_1/T_0 =3.98 are shown for the case with $L \neq 0$.

significant, which drastically slows down the heating of the surface. Subsurface heated layer is formed at this stage. Then, the ablation front catches up with the heated layer, which is reflected by the gradual decrease in $\ell(t)$. When the ablation velocity is big enough, the surface temperature and the ablation rate sharply increase. This corresponds to the partial ablation of the overheated subsurface layer, which exists due to the positive thermal gradient (2.5a). Finally, after the end of the pulse, the surface cools down due to the heat conduction and post-pulse ablation occurs. Due to the condition $\alpha^2 D\tau << 1$ the cooling is slow and significant amount of material is ablated after the pulse. For the numbers employed in Fig. 11 ablation ceases only at $\alpha^2 Dt \approx$ 1-10.

The time to reach the "second threshold" - i.e., the sharp increase in T_s and v can be estimated as the time to heat the layer of thickness ~$1/\alpha$ (see, e.g. [4]):

$$t_2 \approx 1/\alpha v \approx (L + H_{gs})/\alpha AI \Rightarrow \phi_2 \approx It_2 \approx (L + H_{gs})/\alpha A \qquad (6.2)$$

When the fluence $\phi > \phi_2$, the second threshold is reached during the pulse. The thickness $h(\phi_2) \approx 1/\alpha$ is ablated with this fluence. Interestingly enough, despite significant differences in the ablation process, with constant material parameters, second threshold is only weakly reflected in the ablation curve $h(\phi)$ (Fig. 11 b). The reason is, that ablation of the overheated layer may occur *after* the pulse as well. With $\phi < \phi_2$, ℓ is larger when the pulse is finished, overheated layer is thicker, it cools down slower, and a larger fraction of the material is ablated after the pulse. The possibility of after the pulse ablation was first discussed in [29]. Our consideration shows, that this effect is reflected weakly on the ablation curves. For rectangular

pulses it is somewhat more pronounced. In reality, the change in ablation curves may be more significant due to temperature dependence of parameters. If, for example, absorptivity A even moderately depends on T_s, the change in the slope of the ablation curve at ϕ_2 may be quite significant according to (4.5), because $T_{s\,max}$ may change almost twice in a narrow fluence interval near ϕ_2 (Fig. 11).

Another feature, exhibited by Fig. 11, is that (4.5) significantly overestimates ϕ_{th} and T_v. The reason is, that in this case the ablation takes place mainly *after* the pulse, and it is erroneous to use t_{FWHM} in the estimations (4.6). In the limiting case when one can neglect the influence of ablation onto cooling process, the material cools down according to (3.2) with $I\equiv 0$, $v=0$. This, with the *constant parameters*, leads to the solution

$$(\alpha\,\ell)^2/2+\alpha\,\ell-\ln(1+\alpha\,\ell)=\alpha^2 Dt\ ,\quad H_s=A\alpha\phi/(1+\alpha\,\ell) \tag{6.3}$$

To estimate ablated depth in the Arrhenius region, one has to integrate the velocity of surface recession over time. Assuming rather high activation temperature, and $H_g \equiv H$, we can use only initial stage of cooling in (6.3), which results in $\ell=(Dt)^{1/2}$ (with big times $\ell \approx (2Dt)^{1/2}$), and use Frank-Kamenetsky expansion (saddle point method) for the integration of Arrhenius exponent

$$h=\int_0^\infty v(t)dt\approx v_0\int_0^\infty \exp\left[-T_a\Big/\left(T_0+\frac{\theta_s}{1+\alpha(Dt)^{1/2}}\right)\right]dt\approx v_0\exp\left[-\frac{T_a}{T_s}\right]\int_0^\infty \exp\left[-\frac{T_a\theta_s\alpha\,(Dt)^{1/2}}{T_s^{\,2}}\right]dt=$$

$$=\frac{2\,v_0}{\alpha^2 D}\left[\frac{T_s^{\,2}}{T_a\theta_s}\right]^2\exp\left[-\frac{T_a}{T_s}\right],\qquad T_s\equiv T_0+\theta_s=T_0+\frac{A\alpha\phi}{c\rho} \tag{6.4}$$

Here, θ_s is the temperature rise just after the end of the laser pulse. In analogy with (4.4)-(4.5) the turnover between the Arrhenius and linear region occurs if the energy spent on ablation constitutes about one half of the absorbed laser fluence.

$$h\left[L+H_g(T_s)\right]\approx A\phi/2 \tag{6.5}$$

where h should be taken from (6.4). This yields the expression for the "first threshold" ϕ_1 and corresponding temperature T_1, indicated in Fig. 11 and in the figure caption. Strong Arrhenius dependence in (6.4) makes ϕ_1 about proportional to $c\rho T_a/A\alpha$ and much less sensitive to other parameters.

Figure 11 reveals, that with $\phi>\phi_1$, the increase in ablated depth with fluence is close to linear with the slope close to that given by (4.5). The existence of the second threshold is entirely due to vaporization enthalpy L, as demonstrated by the $T_s(\phi)$ curve with $L = 0$, which shows smooth behavior. This is because with $L = 0$ surface temperature gradient is zero and subsurface heated layer is not formed.

As in Fig. 9, ablation curves are less steep at higher fluences, and approximations (4.5)-(4.7) work even worse for weakly absorbing materials with $L=0$. In this region no analytical formulas exist and method of moments provides indispensable tool especially in the case when cooling and after-pulse ablation proceed at comparable rates, as it is often the case with polymers [7]. The overall behavior of ablation curve is faster than logarithmic but slower than linear. Logarithmic inset shows, that especially with $L = 0$, $\log(h)$ vs. ϕ dependence at moderate fluences may look as linear one, which bends up at elevated fluences. This was observed in many experiments on polymer ablation [5, 8, 28].

The method of moments works in the case of temperature dependent parameters as well. More detailed studies of this case, which should include modifications due to possible $\alpha(T)$ dependence will be considered in a separate paper.

7. SINGLE-PULSE ABLATION OF POLYIMIDE

Figure 12 shows the application of developed technique to the analysis of the single-pulse ablation of Polyimide (Kapton^{TM} H) by 248 and 308 nm excimer laser pulses [30] . The fit of Arrhenius tails with known temperature dependences of thermophysical parameters allows one to find the activation energy and preexponential factor in the expression for the evaporation rate (2.4). The part of the ablation curves at higher fluences should be fitted by varying L and attenuation coefficient for the plume α_g . Here the fit is ambiguous, since increase in both of these parameters decreases the slope of the ablation curves. Thus, reasonable fit may be provided with different pairs of these quantities. This ambiguity should be eliminated by the consideration of wider range of fluences and/or pulse duration. This is the prospect for further work.

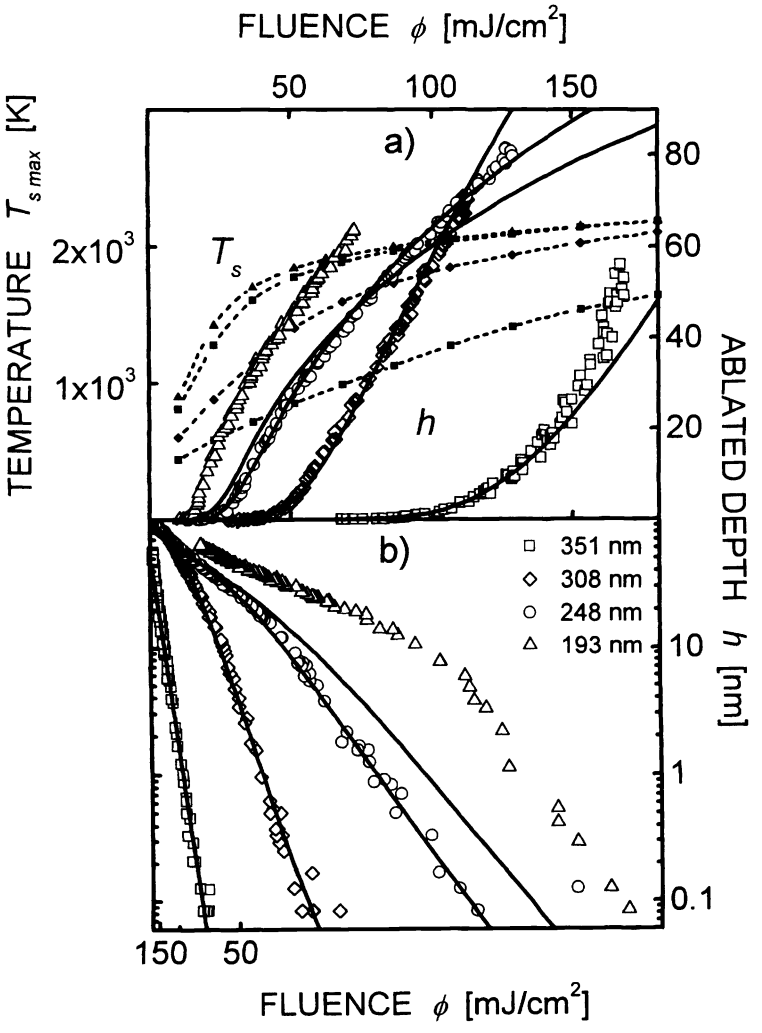

Fig. 12. Modeling of the single-pulse ablation of PI with the moments technique. $\tau = 6.13$ ns ($t_{FWHM} = 15$ ns), $A = 0.89$, $\alpha = 0.86\times10^5$ cm^{-1}, $v_0 = 10^6$ cm/s, $T_a = 18000$ K $\equiv 1.55$ eV, $T_0 = 300$ K, c is given by (5.3) with $c_0 = 0.96$, $c_\infty = 2.55$ J/gK, $T_c = 460$ K, $c_g = 2.55$ J/gK, K is given by (5.4) with $K_0 = 1.55\times10^{-3}$ W/cmK, $n = 0.28$, $\rho = 1.42$ g/cm^3, $L/\rho = 0.7$ kJ/g. **a)** Kinetic curves in "normal"coordinates: h vs. fluence. **b)** Kinetic curves in Arrhenius coordinates: log (h) vs. inverse fluence.

8. CONCLUSIONS

We studied the influence of different factors onto ablation kinetics (ablated depth h vs. fluence ϕ) within the frame of thermal model. Calculations were done on the basis of the method of moments. This study shows that one can distinguish three characteristic regions of fluences: i) Arrhenius region, where laser energy mainly goes to the heating of the material; ii) Linear region, where the ablated depth increases linearly with fluence due to overall energy balance; and iii) Screening region, where shielding of the incoming radiation by the ablation products plays an important role. The analytical formulas are obtained.

Small vaporization enthalpy results in a sub-linear $h(\phi)$ dependence, which, nevertheless, remains faster than logarithmic. This may explain the increase in slope in log (h) vs. ϕ dependencies observed in many experiments.

With weakly absorbing materials ablation may proceed in two significantly different regimes -- without or with ablation of the heated subsurface layer. The latter occurs at higher fluences and reveals significantly higher ablation temperatures. Ablation of the subsurface layer may occur after the laser pulse as well.

As an illustrative example, the method of moments was applied to the quantitative analysis of the single pulse ablation curves of polyimide. This analysis confirms the statements[30] about thermal mechanism of ablation.

Acknowledgments:

The authors are grateful to the Russian Basic Research Foundation and the "Fonds zur Förderung der wissenschaftlichen Forschung in Österreich" for financial support. Part of this work was supported by INTAS grant.

References

1. D. Bäuerle, "*Laser Processing and Chemistry*", 2nd ed. Springer-Verlag, Berlin, Heidelberg, 1996.
2. E. Fogarassy, D. Geohegan, M. Stuke (eds), "*Laser Ablation*", North-Holland, Amsterdam, 1996.
3. E. Fogarassy, S. Lazare (eds), "*Laser Ablation of Electronic Materials*", North-Holland, Amsterdam 1992.
4. S. I. Anisimov, V. A. Khokhlov, "*Instabilities in Laser-Matter Interaction*", CRC Press, Boca Raton 1995.
5. R. Srinivasan, B. Braren, *Chem. Rev.* **89**, p.1303 (1989)
6. N. P. Furzikov, *Appl. Phys. Lett.* **56**, p.1638 (1990)
7. S. R. Cain, F. C. Burns, C. E. Otis, B. Braren: *J. Appl. Phys.* **72**, p.5172 (1993)
8. S. Lazare, V. Granier: *Laser Chem.* **10**, p.25 (1989)
9. M. I. Bessonov, "*Polyimides - a Class of Thermally stable Polymers*", NASA Technical Memorandum, Washington DC 20546, 1986;
   J. Guillet: "*Polymers - Photophysics and Photochemistry. An Introduction to the Study of Photoprocesses in Macromolecules*", Cambridge University Press, 1985
10. B. Luk'yanchuk, N. Bityurin, M. Himmelbauer, N. Arnold, *Nucl. Instrum. Meth.* B **122**, p.347 (1997)
11. D. Zwillinger, "*Handbook of Differential Equations*", Academic Press, Boston, 1989;
    N.V.Karlov, N.A.Kirichenko, B.S.Luk`yanchuk, "*Laser Thermochemistry*", Cambridge Interscience Press 1997
12. S. I. Anisimov, Ya. A. Imas, G. S. Romanov, Yu. V. Khodyko, "*Action of High -Power Radiation on Metals*", National Technical Information Service, Springfield, Virginia, 1971.
13. B. Luk'yanchuk, N. Bityurin, S. Anisimov, N. Arnold, D. Bäuerle: *Appl. Phys.* A **62**, p. 397 (1996)
14. P. P. Pronko, S. K. Dutta, D. Du, R. K. Singh, *J. Appl. Phys.* **78** (10), p.6233 (1995)
15. S. Fähler, H.-U. Krebs, *Appl. Surf. Sci.*, **96-98**, p. 61 (1996)
16. X. Mao, W.-T. Chan, M. Caetano, M. A. Shannon, and R. E. Russo, *Appl. Surf. Sci.*, **96-98,** p.126 (1996)
17. A. Peterlongo, A. Miotello, R. Kelly, *Phys. Rev.* **E 50** (6), p.4716 (1994)
18. N. Arnold, B.Luk'yanchuk, N.Bityurin, D. Bäuerle: *Laser Physics* **8**, No.1 (1998); *Applied Surface Science* (1998)
19. S. Wolfram: "*Mathematica*", Second Edition, Addison-Wesley Publishing Company, Inc., 1991.
20. H. H. G. Jellinek, R. Srinivasan, *J. Phys. Chem.* **88**, p. 3048 (1984)
21. S. V. Babu, G. C. D'Couto, F. D. Egitto, *J. Appl. Phys.* **72**(2), p.692 (1992)
22. V. N. Tokarev, J. G. Lunney, W. Marine, M. Sentis, *J. Appl. Phys.* **78** (2), p.1241 (1995)

23. D. E. Gray (ed.), "*American Institute of Physics Handbook*", 3d Ed., McGraw-Hill, 1973.
24. "*JANAF Thermochemical Tables*", National Bureau of Standards, USA, 1970.
25. Y. B. Zeldovich, Yu. P. Raizer: "*Physics of Shock Waves and High-Temperature Hydrodynamic Phenomena*", eds. W. D. Hayes and R. F. Probstein, Academic Press, London, 1966.
26. V. L. Ginzburg, "*The Propagation of Electromagnetic Waves in Plasmas*", 2nd ed. Pergamon, Oxford, 1970.
27. R. K. Singh, *Journal of Electronic Materials*, **25,** p. 125 (1996)
28. R. Srinivasan: In "*Interaction of Laser Radiation with Organic Polymers*", Ed. by J. C. Miller, Springer Series in Materials Science **28** Springer-Verlag, 1994, p.107
29. D. Bäuerle, B. Luk'yanchuk, P. Schwab, X. Z. Wang, E. Arenholz: in "*Laser Ablation of Electronic Materials - Basic Mechanisms and Applications*", eds. E. Fogarassy and S. Lazare, Elsevier, Amsterdam 1992, p. 39
30. S. Küper, J. Brannon, K. Brannon: *Appl. Phys.* A **56**, p.43 (1993)

Further author information -
N.A. (correspondence): Phone: ++43 732 2468-9243 / Fax: 9242, E-Mail: nikita.arnold@jk.uni-linz.ac.at
B.L.: E-Mail: lukyanch@kapella.gpi.ru N.B.: E-Mail: bit@appl.sci-nnov.ru D.B.: E-Mail: dieter.baeuerle@jk.uni-linz.ac.at